Influence of Lithium Sulfide Weight Ratio on Optical and Electrical Properties of Blend Solid Electrolytes Based on Chitosan/Polyvinylpyrrolidone

Alaa M. Qusay
Mohammed K. Jawad

Department of Physics,
College of Science,
University of Baghdad,
Baghdad, IRAQ

The most popular electrochemical energy storage technology in the future will be solid-state lithium batteries, which have a high energy density, a small size, can work in a wide range of temperatures, and are easy to picaresque to produce biocompatible chitosan/polyvinylpyrrolidone (CS:PVP) polymer blends at a constant weight ratio of 50:50 with different lithium sulfide proportions. The synthesized samples were tested using FTIR, UV-visible, and alternating current conductivity. FTIR showed two peaks, confirming chitosan and PVP. Adding lithium and sulfide ions changed the polymer matrix hydrogen bonding network. The material's electrical structure changed when lithium sulfide content increased because UV-visible spectroscopy showed the optical bandgap narrowed. Lithium sulfide salt improved electronics, especially ionic conductivity. Highest ionic conductivity (2.9×10^{-3} S/cm) was achieved at 37.5 wt.% lithium sulfide concentration at ambient temperature, highlighting its potential in advanced solid-state battery technologies.

***Keywords*:** Li_2S salt; Chitosan; Polyvinyl pyrrolidone; Solution casting method
Received: 21 December 2024; **Revised:** 21 February; **Accepted:** 28 February 2025

1. Introduction

Over the past two decades, the increasing demand for portable communications gadgets, laptops, and hybrid electric cars has triggered a paradigm change in lithium battery development [1]. Due to its numerous advantages, high energy density, extended cycle life, and memory effect. Since they were first sold in 1991, the density of energy stored in lithium-ion batteries (LIBs) increased significantly. Researchers and developers are creating better active electrode materials, more efficient electrolytes, and the best ways to build cells [2]. The electrolytes employed in conventional lithium-ion batteries are organic liquids characterized by high ionic conductivity; the efficiency of lithium-ion batteries is influenced by their flammable characteristics, posing a significant safety risk. The increased safety, ease of manufacturing, and superior flexibility of solid polymer electrolytes have made them a popular replacement for liquid electrolytes [3]. Consumer electronics have shifted their focus to lithium-ion batteries (LIBs) because of their superior performance and remarkable cost-effectiveness. The electrolyte, cathode, anode, and separator are the four primary parts of a conventional lithium-ion battery. Among the many essential components of a LIB, the electrolyte has a significant impact on the safety, capacity, and operational aspects of the cycle [4]. In the past three decades, considerable attention has been directed into polymer electrolytes and their potential application in rechargeable lithium-ion batteries [5]. Chitosan is characterized by its linear polysaccharide structure and is a widely used natural polymer. Chitosan, a derivative of chitin with a high concentration of N-acetyl, is another remarkable discovery. The industrial and biological applications of chitosan have led to its recent extensive utilization. Physicochemical changes, such as mechanochemical disorganization, plasma treatment for amorphization, and copolymerization, can make properties of chitosan very different [6]. A highly effective method for obtaining novel materials for film production is blending [7]. The decisive factor for the choice was the excellent optical, mechanical, and electrical properties of polyvinyl pyrrolidone (PVP). PVP is compatible with various materials and quickly produces films with a high specific surface area. Organic solvents and distilled water are optimal ideal for dissolving PVP. Low scattering loss improves the optical application possibilities and leads to better dispersion and surface formation [8]. The electrochemistry community has long been interested in Li/S technology [9]. Li-S batteries (LSBs) offer advantages compared to Li-ion batteries (LIBs), but also present unique challenges. Other important features include lifespan, Coulomb efficiency (CE), and self-discharge, which is a new enable era in electric car technology and energy storage on the grid [10]. The aim of the work investigates how lithium sulfide concentration weight ratio on optical and ionic conductivity.

2. Experimental Part

Chitosan (Cs) with medium molecular weight (75-85% deacetylate), chemical formula $(C_2H_4O)_n$, the exporter's laboratory compounds were supplied by Alpha Chemika India and used to produce an extra specially purified product, with a degree of

deacetylation of 86%. Polyvinylpyrrolidone (PVP) (MW 40.000, purity> 99%) was supplied by Sigma Aldrich Cchemicals Ltd., India. Lithium sulfide (Li_2S) has a molecular weight of 45.95, a specific heat of 938°C, a boiling point of 1372°C, and a powdery appearance, was supplied by Sigma Aldrich. Iodine (I_2) of molecular weight 253.81 g/mol was supplied by BDH Limited Poole England.

The solution casting method used to fabricate the samples was tabulated in table (1). A fixed ratio (CS:PVP) of 50:50 was used, and the amounts of Li_2S were 7.5, 15, 22.5, 30, 37.5 %, and I_2 with a salt content of 10 wt.%. The first step was to dissolve 0.5 g of CS in 40 mL of distilled water containing 1% acetic acid. The mixture was brought to 50 °C and continuously stirred using a magnetic stirrer for approximately 5 hours. In comparison, 0.5 g of PVP polymer was dissolved in 5 mL of distilled water containing 1% acetic acid. The PVP solution was added to the CS solution and continuously stirred for 2 hours until a homogeneous aqueous solution was obtained. The next step was to dissolve Li_2S and I_2 in 5 mL of dimethyl sulfoxide (DMSO) in a glass vessel. The mixture was stirred continuously for 15 min using a magnetic stirrer. The synthesized mixture (Li_2S:I_2) was gradually added to the polymer blend and stirred continuously for at least 10 hours. Films containing different amounts of Li_2S and I_2 salts were prepared using the same methods. Finally, the solution mixture was applied to several dry plastic Petri dishes and evaporated to form a dry, solid film.

3. Results and Discussion

Fourier-transform infrared (FTIR) spectroscopy is a crucial tool in modern analytical chemistry and is widely used to examine various vehicles by elucidating their complex chemical structures and functional groups. This is highly beneficial for understanding the complex chemical composition, bond configurations and structural properties of materials. The understanding and manipulating the materials underlying modern technologies and industries depend significantly on FTIR. All aspects have been carried out with great attention to detail, from polymer characterization to material composition analysis to monitor the quality control process [11]. The FTIR result of polymer blends (CS:PVP) was obtained, as shown in Fig. (1) and table (2). The presence of hydroxyl groups ($^-$OH), likely produced from chitosan, is demonstrated by the prominent peak at 3261.63 cm^{-1}. The C=O stretching vibration of PVP, peaking at 1647.21 cm^{-1}, identifies one of the related functional groups [12]. This bond links the symmetrical stretching vibrations of CH to the peaks at 2926.01 and 2856.58 cm^{-1}, respectively [13]. The deformation mode of the C-H symmetric group is responsible for the sharp peaks at 1371.39 and 1421.54 cm^{-1}, while C-O stretching vibration in chitosan is responsible for the broad peaks at 1056.99 and 1018.41 cm^{-1}. The C=O-NH group was associated with a high absorption at 1560.41 cm^{-1} [14]. The peaks at 948.98 and 839.03 cm^{-1} are in agreement to the stretching of C-O and the rocking of CH_2, respectively [15]. The separate peaks indicate that the chitosan and PVP molecules have interacted and formed a combination.

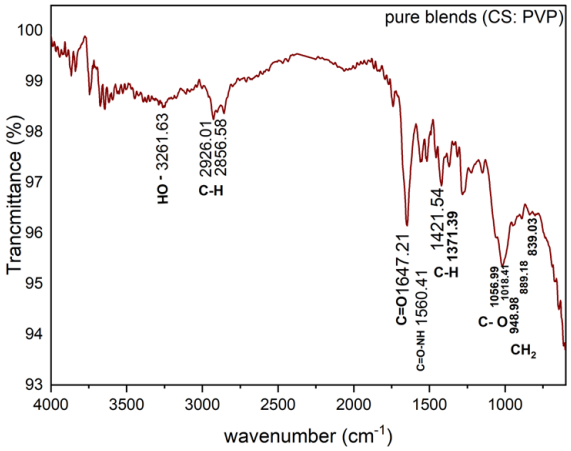

Fig. (1) FTIR spectrum of pure blends (CS:PVP)

Table (2) Bands type and energies for pure blends (CS:PVP) with different ratio of Li_2S

Band Type	CS:PVP	CS:PVP:Li_2S
O-H	3261.63	3419.72
C-H	2926.01 2856.58	-
C=O	1647.21	1668.43
C=O-NH	1560.41	-
C-H	948.98 - 839.03	-
CH_2	-	1313.52

Figure (2) shows the FTIR spectrum of samples B1, B2, B3, B4, and B5 containing a mixture of CS:PVP with different weight percentages of Li_2S. The stretching vibration of the hydroxyl bond accounts for the broad band observed at around 3419.72 cm^{-1}. The increased intensity of these peaks due to the addition of PVP and further deepening by Li_2S suggests interactions between Li^+ ions and the hydroxyl groups of the carbonyl groups of PVP [16]. The characterized swath of chitosan suggests that hydrogen bonds may exist between PVP and CS., which is located at 1668.43 cm^{-1}. The peak 1668.43 cm^{-1} is indicative of the elongation of the carbonyl set C=O. Additionally, with regard to the CH alteration phases of the CH_2 group are the peaks at 1313.52 cm^{-1} [17].

The analysis of the significance of optical characteristics in the visible and ultraviolet spectra, including band gap energy (E_g) and polymer composites, is facilitated by UV-visible spectroscopy. and other optical features can be easily determined from UV-visible spectroscopic measurements in the range 200-1100 nm [18]. The UV/visible spectroscopy has emerged as a significant tool for estimating

polymers' optical gap energy. An association between the optical absorption edge and the optical gap energy may be established using Tauc's equation (Eq. 1). By extrapolating the spectrum and identifying its intersection with the abscissa, we can determine the optical gap energy (E_g). Tauc's equation, essential for this analysis, is provided as [19]

$$\sigma h\upsilon = A\left(h\upsilon - E_g\right)^2 \quad (1)$$

where h is Planck's constant, ν is the photon's frequency, α is the absorption coefficient, and A is a proportionality constant [20]

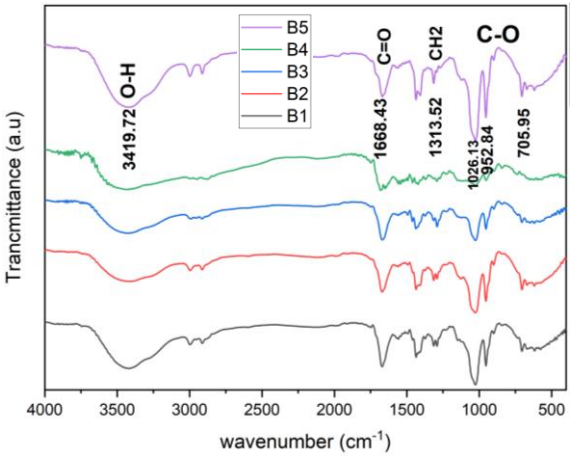

Fig. (2) FTIR spectra of pure blends (CS:PVP) with different ratio of Li_2S

Due to reach saturation. The E_g values for A0-A5 with and without wt.% Li_2S are display in Fig. (3) and table (3). The optical energy gap values are contingent upon the weight percentage of Li_2S, which leads to a decrease in the optical energy gap with an increased Li_2S weight ratio. A smaller bandgap is the outcome of an increase in the shift of the conduction and valence bands and an improvement in carrier-carrier interaction brought about by a high concentration of carriers in these bands.

Table (3) Variation of energy gap of Cs:PVP blends with and without different concentrations of Li_2S

Assignment	E_g (eV)
B0	3.4
B1	3.1
B2	2.5
B3	2.44
B4	2.38
B5	2.03

By analyzing Nyquist plots, one can identify and connect the analogous circuit elements in a way that follows the Nyquist form. As a result, obtaining the AC curve is the first and foremost step in evaluating surface characteristics. The electrical circuit simulation is subsequently used for this purpose (see Fig. 4) [21]. As expected, the system with the lowest Rb concentration maximizes the AC ionic conductivity. As the salt content in the solution increases, the bulk resistance diminishes, and the ionic conductivity enhances. The higher concentration of mobile ions (cation and anion) in the solid electrolytes and the higher rate at which salts break apart improve the conductivity. The AC conductivity has been calculated for all electrolyte systems using the following equation:

$$\sigma = \frac{l}{R_b * S} \quad (2)$$

where l, R_b and S are thickness of film, the resistance of sample, and the mean area of the electrodes [22] as display in Fig. (4) and table (4)

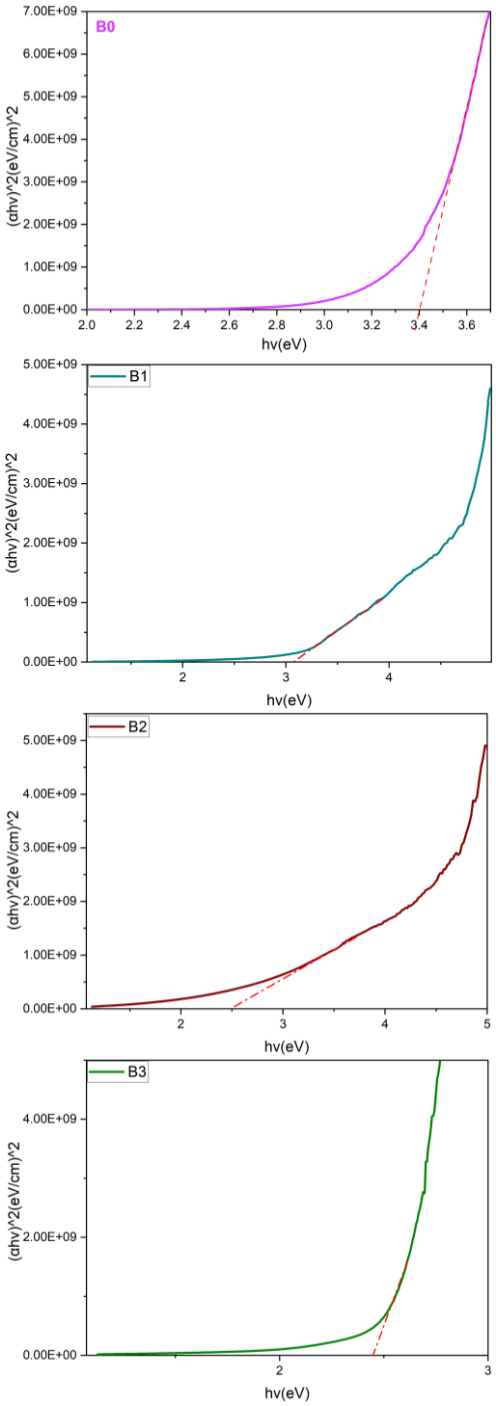

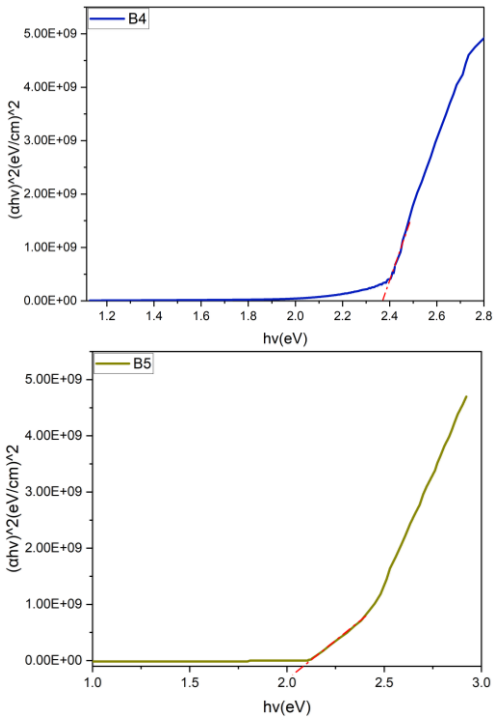

Fig. (3) Relationship between $(\alpha h\nu)^2$ and photon energy (hv) for Cs:PVP mixtures with different weight ratios of Li_2S

Table (4) The ionic conductivity of samples with and without Li_2O at room temperature

Samples	R_b (Ω)	Conductivity (S/cm)
B0	2560000	0.7×10^{-8}
B1	500	6.9×10^{-5}
B2	310	1.12×10^{-4}
B3	100	3.49×10^{-4}
B4	50	6.9×10^{-4}
B5	12	2.9×10^{-3}

The ionic conductivity of the polymers as a function of temperature and Li_2S wt.% is shown in Fig. (5), which describes the increasing ionic conductivity with increasing Li_2S content, reaching a high value at 37.5 wt.%. The ionic conductivity values of the electrolyte B5 (2.9×10^{-3} S.cm^{-1}) at 25 °C. The ions move from a location to another by orbiting the specific oxygen sites of the polymer. At elevated salt concentrations, conductivity saturation can occur due to ion-ion interactions [23]. As the concentration of Li_2S increases, the cluster enlarges, resulting in the significant increase in conductivity, which shows that the ionic conductivity increases when the concentration reaches 37.5% [24].

The study of the interactions between polymer plasticizers and their constitution and ionic mobility is facilitated by dielectric relaxation. Dielectric qualities can be described in various methods, including the terahertz material, relative permittivity, loss tangent, dielectric constant, microwave reflection coefficient, and split post-dielectric resonance technique [25]. The fundamental explanation for the relationship between applied electric field frequency and dielectric constant is the impact of field frequency on material polarization [26].

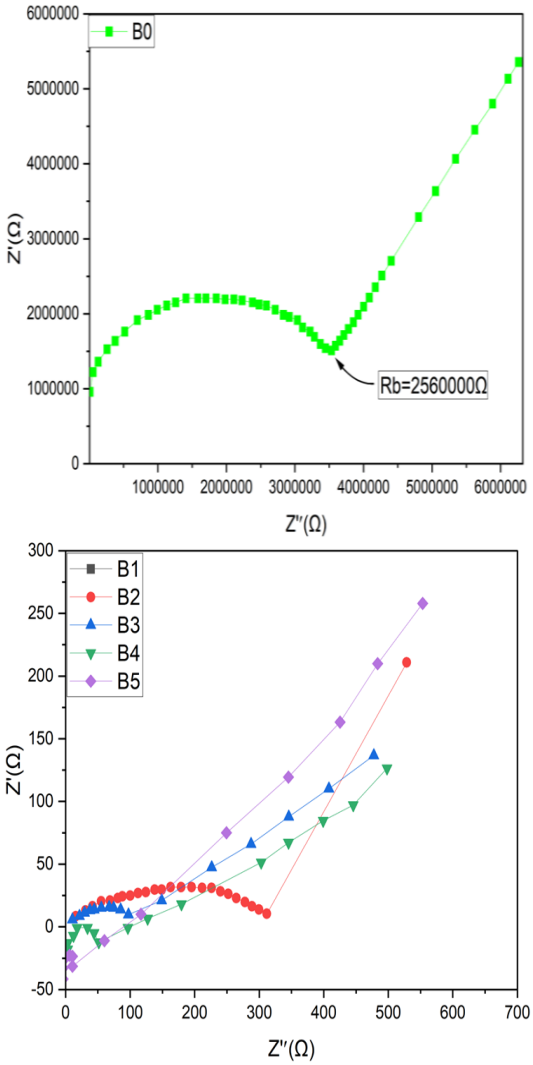

Fig (4) Nyquist plots for pure mixtures and pure mixtures containing different weight percentages of Li_2S

Figure (6) illustrates the relationship between the frequency of the mixed compounds and the true dielectric constant. It demonstrates that the true dielectric constant decreases as the frequency increases; this decrease in the dielectric constant at higher frequencies results from the dielectric dispersion increase. This phenomenon can be attributed to the behavior of polar materials, which initially have high real dielectric values. This can be explained by the fact that dipoles cannot respond to rapid field changes at higher frequencies, in addition to the presence of polarization effects. At higher frequencies, the electric field also experiences rapid periodic reversals due to the absence of excess ion diffusion in the field's direction. Consequently, the dielectric of all samples decreases as the frequency increases [27].

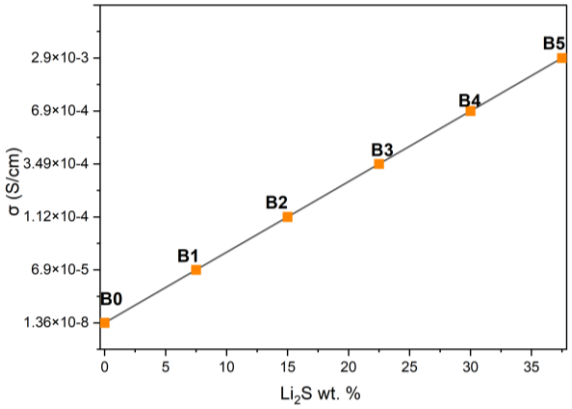

Fig. (5) Electrical conductivity of CS:PVP blend versus salt concentration

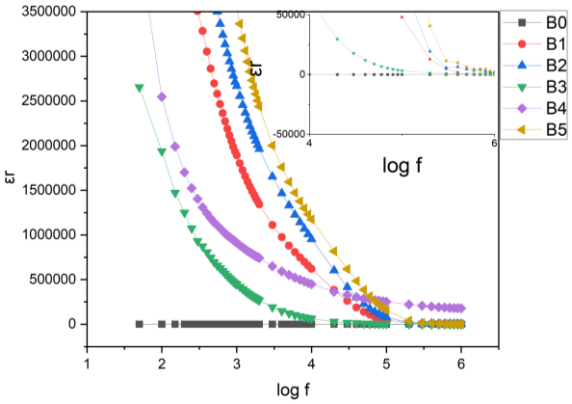

Fig. (6) Dielectric constant (ε_r) versus frequency (Log*f*) for electrolytes (B) with different concentrations of Li_2S

4. Conclusion

There is a significant demand for battery technologies that are characterized by substantial capacities and high energy densities, driven by the increasing prevalence of electric cars and large-scale energy storage systems. A mixture of CS:PVP with certain ratios was fabricated using a solution casting technique with the addition of different weight percent of Li_2S. A significant interaction between the polymer (CS:PVP) and Li_2S was revealed, which causes slight changes in the position of the stretching modes, indicating its effect on the interactions with electrolytes. The energy gap decreased as the proportion of Li_2S salt increased. It was observed that the ionic conductivity increases with increasing salt concentration of Li_2S and the electrolyte B5 contains 37.5% of Li_2S owned highest ionic conductivity 2.9×10^{-3} S/cm. The dielectric constant decreases with increasing frequency for all samples, this behavior being due to the dissociation of ions.

References

[1] A.M. Stephan and K.S. Nahm, "Review on composite polymer electrolytes for lithium Batteries", *Polymer*, 47(16) (2006) 5952-5964.

[2] H. Jia and W. Xu, "Electrolytes for high-voltage lithium batteries", *Trends in Chem.*, 4(7) (2022) 627-642.

[3] S. Mohamadzade et al., "Effect of SiO_2 on the Performance of Cellulose/Poly (Vinylidene Fluoride) Films as Polymer Electrolytes for Lithium Ion Battery", *Chem. Electro. Chem.*, 11(23) (2024) e202400420.

[4] C.M. Costa et al., "Recent advances on separator membranes for lithium-ion battery applications: From porous membranes to solid electrolytes", *Ener. Stor. Mater.*, 22 (2019) 346-375.

[5] E.A. Swady and M.K. Jawad, "Dependency of the AC conductivity of blend nanocomposites on the Lil and ZnO percent", *AIP Conf. Proc.*, 2437 (2022) 020053.

[6] L.A. Jassim and M.K. Jawad, "Physical Properties of Natural Blend Thin Film Composites Reinforced with Nanoparticles", *Iraqi J. Appl. Phys.*, 20(1) (2024) 61-66.

[7] E. Podgorbunskikh et al., "Mechanical Amorphization of Chitosan with Different Molecular Weights", *Polymers*, 14 (2022) 4438.

[8] A.M. El-naggar et al., "Structural, Electrical and Dielectric Characteristics of polypyrrole doped polyvinyl alcohol / carboxymethyl cellulose blended polymer", *J. Indian Chem. Soc.*, 102(4) (2025) 101648.

[9] H. Yamin and E. Peled, "Electrochemistry of a nonaqueous lithium/sulfur cell", *J. Power Sources*, 9, (1983) 281-287.

[10] W. Ni "Perspectives on Advanced Lithium–Sulfur Batteries for Electric Vehicles and Grid-Scale Energy Storage", *Nanomaterials*, 14(12) (2024) 990.

[11] A.H. Kuptsov and G.N. Zhizhin, **"Handbook of Fourier transform Raman and infrared spectra of polymers"**, Elsevier (1998).

[12] L. Doan and K. Tran, "Relationship between the Polymer Blend Using Chitosan, Polyethylene Glycol, Polyvinyl Alcohol, Polyvinylpyrrolidone, and Antimicrobial Activities against Staphylococcus aureus", *Pharmaceutics*, 15(10) (2023) 2453.

[13] F.M. Ahmed and M.K. Jawad, "Characterization of Blend Electrolytes Containing Organic and Inorganic Nanoparticles", *Iraqi J. Appl. Phys.*, 20(1A)
(2024) 43-50.

[14] E.R. Kenawy et al., "Vanillin loaded-physically crosslinked PVA/chitosan/itaconic membranes for topical wound healing applications", *J. Appl. Biomater. Func. Mater.*, 22 (2024).

[15] A.E.T. Zidan et al., "Characterization and some physical studies of PVA/PVP filled with MWCNTs", *J. Mater. Res. Technol.*, 8(1) (2019) 904–913.

[16] A.A. Kareem et al., "Li_2CO_3 as a Modifier for PVA/PVP/PEG Blend Polymer Electrolytes: Effects on Structural Integrity, Electrical Performance, Thermal Behavior and Optical Properties, Polymer-Plastics Technology and Materials", *Polym. Plast. Technol. Mater.*, 64(5) (2025) 735-746.
[17] I.A. Safo et al., "The role of polyvinylpyrrolidone (PVP) as a capping and structure-directing agent in the formation of Pt nanocubes", *Nanoscale Adv.*, 1 (2019) 3095-3106.
[18] L.A. Jassim and M.K. Jawad, "Influence of Incorporating MWCNTs on some Physical Characteristics of Blend Nanocomposites, Influence of Incorporating MWCNTs on Some Physical Characteristics of Blend Nanocomposites", *Iraqi J. Phys.*, 22(1) (2024) 95-105.
[19] N. Balakrishnan et al., "Diversity and Applications of New Age Nanoparticle", IGI Global (2023).
[20] O.R. Fonseca-Cervantes et al., "Effects in Band Gap for Photocatalysis in TiO_2 Support by Adding Gold and Ruthenium", *Processes*, 8(9) (2020) 1032.
[21] H.S. Magar, R.Y.A. Hassan and A. Mulchandani, "Electrochemical Impedance Spectroscopy (EIS): Principles, Construction, and Biosensing Applications", *Sensors*, 21(19) (2021) 6578.
[22] H. Ohno **"Electrochemical Aspects of Ionic Liquids"**, John Wiley & Sons, Inc. (2005).
[23] Zh. Tian et al., "Electrolyte Solvation Structure Design for Sodium Ion Batteries", *Adv. Sci.*, 9(22) (2022) 2201207.
[24] W. Zhang et al., "Experimental and Modeling of Conductivity for Electrolyte Solution Systems", *ACS Omega*, 5(35) (2020) 22465-22474.
[25] J.M. Hadi et al., "Electrochemical Impedance study of Proton Conducting Polymer Electrolytes based on PVC Doped with Thiocyanate and Plasticized with Glycerol", *Int. J. Electrochem. Sci.*, 15 (2020) 4671-4683.
[26] M. Xie et al., "Research progress on porous low dielectric constant materials", *Mater. Sci. Semicond. Process.*, 139 (2022) 106320.
[27] F.M. Ahmed and M.K. Jawad, "Nanocomposites electrolytes based conductive polymer for electrochemical application", *J. Theor. Appl. Phys.*, 18 (2024) Available from: https://oiccpress.com/jtap/article/view/8043.

Table (1) Composition of electrolytes system

Samples	Chitosan (CS)	Acetic Acid	Polyvinylpyrrolidone (PVP)	dimethyl sulfoxide (DMSO)	Lithium Sulfide (Li_2S) %	Iodine (I_2) (g)	dimethyl sulfoxide (DMSO)
B0	0.5	40 ml	0.5	5 ml	0	0.0000	5 ml
B1	0.5	40 ml	0.5	5 ml	7.5	0.0414	5 ml
B2	0.5	40 ml	0.5	5 ml	15	0.0829	5 ml
B3	0.5	40 ml	0.5	5 ml	22.5	0.1243	5 ml
B4	0.5	40 ml	0.5	5 ml	30	0.1657	5 ml
B5	0.5	40 ml	0.5	5 ml	37.5	0.2071	5 ml

